



# DNA polymerase beta modulates cancer progression via enhancing CDH13 expression by promoter demethylation

Meina Wang<sup>1</sup> · Kaili Long<sup>1</sup> · Enjie Li<sup>1</sup> · Lulu Li<sup>1</sup> · Binghua Li<sup>2</sup> · Shusheng Ci<sup>1</sup> · Lingfeng He<sup>1</sup> · Feiyan Pan<sup>1</sup> · Zhigang Hu<sup>1</sup> · Zhigang Guo<sup>1</sup>

Received: 21 April 2020 / Revised: 18 June 2020 / Accepted: 30 June 2020 / Published online: 8 July 2020  
© The Author(s), under exclusive licence to Springer Nature Limited 2020

## Abstract

DNA polymerase  $\beta$  (Pol  $\beta$ ) plays a critical role in DNA base excision repair (BER), which is involved in maintaining genomic stability and in the modulation of DNA demethylation. Numerous studies implicated deficiency of Pol  $\beta$  in the genomic instability and dysregulation of genes expression, leading to affecting initiation of cancer. However, the role of Pol  $\beta$  in cancer progression is still unclear. Here, we show that Pol  $\beta$  depresses migratory and invasive capabilities of both breast and lung carcinomas, which were evident in human breast and lung cancer cells, as well as in mouse xenograft tumors. On the molecular basis, overexpression of Pol  $\beta$  enhanced expression of CDH13, which show function on cell adhesion and migration. Knockdown of CDH13 restores the migratory, invasive capabilities and angiogenesis in tumor, which gets impaired by Pol  $\beta$ . According to the function of BER on modulation of DNA demethylation, our studies on CDH13 expression and the DNA methylation levels of CDH13 promoter suggested that Pol  $\beta$  promotes expression of CDH13 by augmenting DNA demethylation of CDH13 promoter. Our findings elucidated a novel possibility that Pol  $\beta$  impair cancer cell metastasis during cancer progression and shed light on the role of Pol  $\beta$  in cancer therapy.

## Introduction

DNA repair genes play key function in mending damaged DNA and maintaining genomic stability [1]. Dysregulation of DNA repair genes are involved in tumor initiation and affect the response of cells to DNA damaging anticancer treatment [2, 3]. In addition to participating in tumor initiation, accumulating evidence has emerged indicating

that genes involved in DNA damage response, such as *PARP1*, *RAD51*, and *BRAC2*, show functions in cancer progression [4–7]. Metastasis is a crucial characteristic of malignancy during cancer progression, which is responsible for most cancer recurrence and poor prognosis [8]. Cancer metastasis is a multistep cell-biological process in which cancer cells leave the original tumor site and migrate to anatomically distant organ sites via the bloodstream or the lymphatic system, and their subsequent adaptation to foreign tissue microenvironments [9]. However, a direct role of DNA repair genes in the regulation of metastasis, as well as the underlying mechanisms, has not been clarified conclusively.

Cellular metastasis and invasion require tumor cells to alter their ability to adhere to both surrounding cells and the extracellular matrix (ECM) [10]. There are four groups of cell adhesion molecules involved in cell–cell and cell–ECM adhesions: integrins, cadherins, the immunoglobulin superfamily, and selectins [11]. Cell–cell or cell–ECM adhesions in most epithelial cells are formed by cadherins [12]. Cadherins are a family of transmembrane proteins that contain calcium-binding domains. The major functions of cadherins are to dictate the modalities of cell interaction with the microenvironment, and to mediate the organization

**Supplementary information** The online version of this article (<https://doi.org/10.1038/s41388-020-1386-1>) contains supplementary material, which is available to authorized users.

✉ Zhigang Hu  
huzg\_2000@126.com

✉ Zhigang Guo  
guo@nju.edu.cn

<sup>1</sup> Jiangsu Key Laboratory for Molecular and Medical Biotechnology, College of Life Sciences, Nanjing Normal University, Nanjing 210023, China

<sup>2</sup> Department of Hepatobiliary Surgery, The Affiliated Drum Tower Hospital, Medical School of Nanjing University, Nanjing 210008, China

of cytoskeleton and the structural architecture of the cells [13]. Biophysical forces applied by cell–cell or cell–ECM adhesion are translated into the cells by cadherins, and mediate the organization of cytoskeleton and the architecture of the cells [14]. The balance of mechanical interactions at cell–cell junctions and cell–ECM adhesions governs basic processes in epithelial-to-mesenchymal transition, cell migration, and gene regulation [12]. CDH13 (also known as T-cadherin or H-cadherin), a nonclassical member of the cadherin family without intracellular domain, plays a critical role in suppression versus initiation or progression of various tumor types. Overexpression of CDH13 reduces malignant properties in several human cancers [15, 16]. CDH13 is commonly downregulated through promoter methylation in various cancers and aberrant methylation of CDH13 can be a diagnostic biomarker for several kinds of cancers [17, 18].

DNA polymerase beta (Pol  $\beta$ ), a 39 kDa protein encoded by the Pol  $\beta$  gene, is one of the key enzyme in maintaining genomic stability during base excision repair (BER) [3, 19, 20]. It functions with two domains: the N-terminal domain, which is essential for the dRP lyase activity, and the C-terminal domain, which performs the nucleotidyl transferase activity during BER. In addition to the function in BER, knockout of Pol  $\beta$  in mouse embryonic fibroblasts (MEF) cell could initiate cellular transcriptional reprogramming [21]. Moreover, studies by others and us indicate that low catalytic activity of Pol  $\beta$  variants is associated with higher cellular transformation and cancer susceptibility [2, 22, 23]. The Pol  $\beta$  gene copy numbers, as well as Pol  $\beta$  mRNA and/or protein levels are related to cancer pathogenesis and prognosis of several kinds of cancers in patients [24, 25]. Recently, a Pol  $\beta$  mutation (T889C) has been reported to be associated with higher incidence of intraperitoneal metastasis in gastric cancer [26], whereas the mechanism is unclear.

In the present study, we identified that elevated expression of Pol  $\beta$  impaired the motility and invasiveness of cancer cells *in vitro*. Pol  $\beta$  overexpression inhibited the tumor invasion and metastasis in a mouse xenograft assay. Notably, we demonstrated that the functions of Pol  $\beta$  on suppression of tumor metastasis are achieved through the Pol  $\beta$ -mediated transcriptional upregulation of CDH13. Moreover, knockdown of CDH13 restored the angiogenesis that was impaired by overexpression of Pol  $\beta$  in mouse xenograft tumors, implicating the role of Pol  $\beta$ /CDH13 axis in tumor angiogenesis and metastasis. According to the key role of Pol  $\beta$  in BER involved in DNA demethylation, Pol  $\beta$  upregulated CDH13 expression via attenuated CDH13 promoter DNA methylation. Collectively, our results not only uncover a novel mechanism by which Pol  $\beta$  suppress tumor metastasis but also suggest the potential of Pol  $\beta$  as a transcriptional effector to regulate other genes implicated in the progression of cancer.

## Results

### Pol $\beta$ is associated with cancer progression and regulates cancer cells motility

To evaluate the relation of Pol  $\beta$  expression and prognosis of cancer patients, we analyzed the expression levels of Pol  $\beta$  in cancer samples according to The Cancer Genome Atlas database. We identified that Pol  $\beta$  was highly expressed in breast cancer tissues and lung cancer tissues compared with adjacent normal tissue (Fig. S1a, b). The immunohistochemistry (IHC) results of normal tissue and tumor tissue showed similar results that higher Pol  $\beta$  expressions were observed in tumor tissues compared with those in normal tissues (Fig. 1a, b). Interestingly, low expression of Pol  $\beta$  was related to the malignancy of breast and lung cancers during cancer progression in cancer tissue samples with or without lymph node metastasis using tissue array analysis (Fig. 1a, b). In breast cancer, 65% of samples from patients without lymph node metastasis (N0) showed high expression of Pol  $\beta$ . Similar result was obtained in lung cancer samples, in which 52% of samples without lymph node metastasis had high expression of Pol  $\beta$  (Fig. S1c, d). Our data showed that the expression level of Pol  $\beta$  was lower in both breast cancer samples and lung cancer samples with lymph node metastasis compared with no metastasis samples. Kaplan–Meier survival analysis showed that lower Pol  $\beta$  expression had poor prognoses in both breast cancer and lung cancer patients (Fig. S1e, f).

Both MCF-7 cells (epithelial cell from human breast adenocarcinoma) and A549 cells (epithelial cell from human lung carcinoma) were widely applied in the studies of cancer cell invasion and migration [27, 28]. Previous studies have verified that Pol  $\beta$  plays a role in cancer development and therapy in MCF-7 and A549 cells [3, 29]. To investigate the effect of Pol  $\beta$  on cancer cell motility, we constructed Pol  $\beta$ -overexpressing MCF-7 and A549 stable cell lines, respectively (Fig. S2a). We found that no difference in cell cycle or apoptosis between overexpressed Pol  $\beta$  and vector cells (Fig. S2b, c). Wound healing assay indicated lower migration in both Pol  $\beta$ -overexpressing A549 and MCF-7 cells compared with cells transfected with empty vector (Fig. 1c, d). Consistently, transwell assay showed that overexpression of Pol  $\beta$  significantly reduced cell migration in both MCF-7 and A549 cells (Fig. 1e). The cortical actin cytoskeleton, which is central to cancer cell motility [30], was reduced in the Pol  $\beta$ -overexpressing cells (Fig. 1f). Furthermore, Pol  $\beta$ -overexpressing MCF-7 and A549 cells showed less invasive growth pattern compared with control cells cultured in three-dimensional matrigel (Fig. 1g). Invasion assay demonstrated that overexpression of Pol  $\beta$  impeded the invasive activity of both MCF-7 and A549 cancer cells (Fig. 1h). Thus, these results suggested

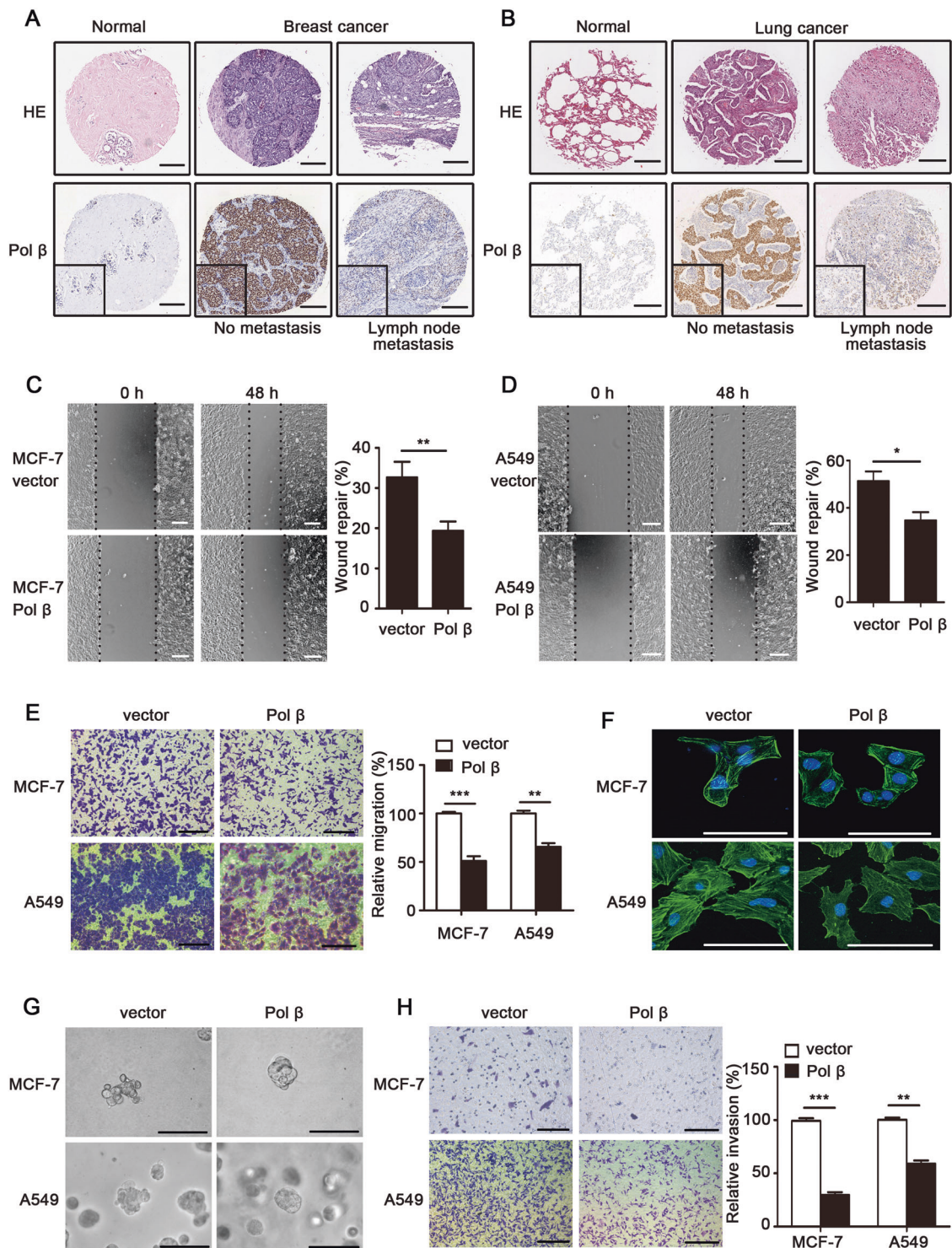


**Fig. 1 Pol  $\beta$  expression correlates with cancer progression and cancer cells motility.** Representative images of HE staining and (IHC) staining of Pol  $\beta$  in normal tissues, tumor tissues of breast tumor (a) and lung tumor (b). Black bar represents 200  $\mu$ m. Wound healing assay in vector and Pol  $\beta$  overexpressing MCF-7 (c) and A549 (d) cells. Images were taken 0 and 48 h after wound formation. The quantitative results of wound healing assay are shown in the right part. The percentage shows wound healing at 48 h compared with 0 h (\*\* $P < 0.01$ , by Student's  $t$  test). e Representative

images of transwell assay for cell migration in MCF-7 and A549 cells. The right part shows the relative percentage compared with vector control (\*\* $P < 0.01$ , by Student's  $t$  test). f Actin stained with phalloidin (green) showed cell spreading in vector or Pol  $\beta$  overexpressing MCF-7 and A549 cells. g 3D matrigel assay tested invasive phenotype of breast and lung cancer cells. h Cell invasion is tested by transwell assay (left panel) and expressed as a relative percentage compared with vector control (\*\* $P < 0.01$ , by Student's  $t$  test).



that high level of Pol  $\beta$  inhibited migration and invasion of cancer cells.

### Overexpression of Pol $\beta$ suppresses tumor invasion and metastasis in vivo

Next, we assessed the effect of Pol  $\beta$  on tumors invasion and metastasis in vivo. MCF-7 cells overexpressing either Pol  $\beta$  or control vector were subcutaneously implanted into nude mice. The tumor sizes were monitored every 3 days. Our data showed that Pol  $\beta$ -overexpressing tumors had a significantly slower growth rate compared with control tumors (Fig. 2a). The final weights of tumors derived from Pol  $\beta$ -overexpressing MCF-7 cells were lower than tumors derived from control MCF-7 cells (Fig. 2b). Moreover, the tumors derived from Pol  $\beta$ -overexpression MCF-7 cells showed substantially reduced local invasion (Fig. 2c) and less angiogenesis (Fig. S3).

To further evaluate the effect of Pol  $\beta$  on tumor metastasis, we constructed mouse models of lung cancer by injecting luciferase-labeled A549 cells with/without overexpression of Pol  $\beta$  into severe combined immunodeficiency (SCID) mice via tail vein. Tumor morphology was assessed by bioluminescent imaging. Overexpression of Pol  $\beta$  resulted in poorer signal compared with control group (Fig. 2d). Furthermore, we identified more extravasation

and invasion of lung cancer sites in the mouse model derived from control A549 cells compared with Pol  $\beta$ -overexpressing A549 cells (Fig. 2e). These data indicated that Pol  $\beta$  steady state level played a critical role in cancer invasiveness and metastasis.

### Pol $\beta$ deficiency enhances tumor metastasis

As overexpression of Pol  $\beta$  protected against tumor invasiveness and metastasis, we investigated whether Pol  $\beta$  deficiency can enhance tumor metastasis and invasion. We knocked down Pol  $\beta$  in MCF-7 and A549 cells by shRNA (Fig. 3a and Fig. S4). These results were supported by the transwell assay in which reduced Pol  $\beta$  observably promoted the migration and invasiveness of MCF-7 and A549 cells (Fig. 3b, c). In addition, increased actin fibers were detected in the Pol  $\beta$  deficiency MCF-7 and A549 cancer cells (Fig. 3d). Furthermore, xenograft tumors derived from Pol  $\beta$  deficiency MCF-7 cancer cells showed higher growth rate and augmented local invasion (Fig. 3e, f). Moreover, we injected luciferase-labeled A549 cells into SCID mice via tail vein and observed that knockdown of Pol  $\beta$  results in more extravasation and colonization of cancer cells in the lung of mice model (Fig. 3g). Collectively, our data revealed that deficiency of Pol  $\beta$  promoted tumor metastasis and invasion in vivo.

**Fig. 2 Pol  $\beta$  depresses tumor metastasis and invasion in in xenograft mouse model. a** MCF-7 cells containing vector or expressing Pol  $\beta$  were injected subcutaneously. Tumor growth were measured every 3 days ( $n = 10$ ) ( $*P < 0.05$ , by Student's  $t$  test). **b** Tumor weight was assessed at 4 weeks after injection ( $*P < 0.05$ , by Student's  $t$  test). **c** Tumors were collected and stained with HE to test tumor invasion. **d** Representative bioluminescent (BLI) images of SCID mice after intravenous injection with A549-vector and A549 overexpression Pol  $\beta$  cells. Heat map indicate intensity of bioluminescence from low (blue) to high (red) ( $n = 5$ ). **e** In left part, representative images show activity of luciferase in lungs from SCID mice as in **d**. The right part shows quantification of lung bioluminescence ( $**P < 0.01$ , by Student's  $t$  test).

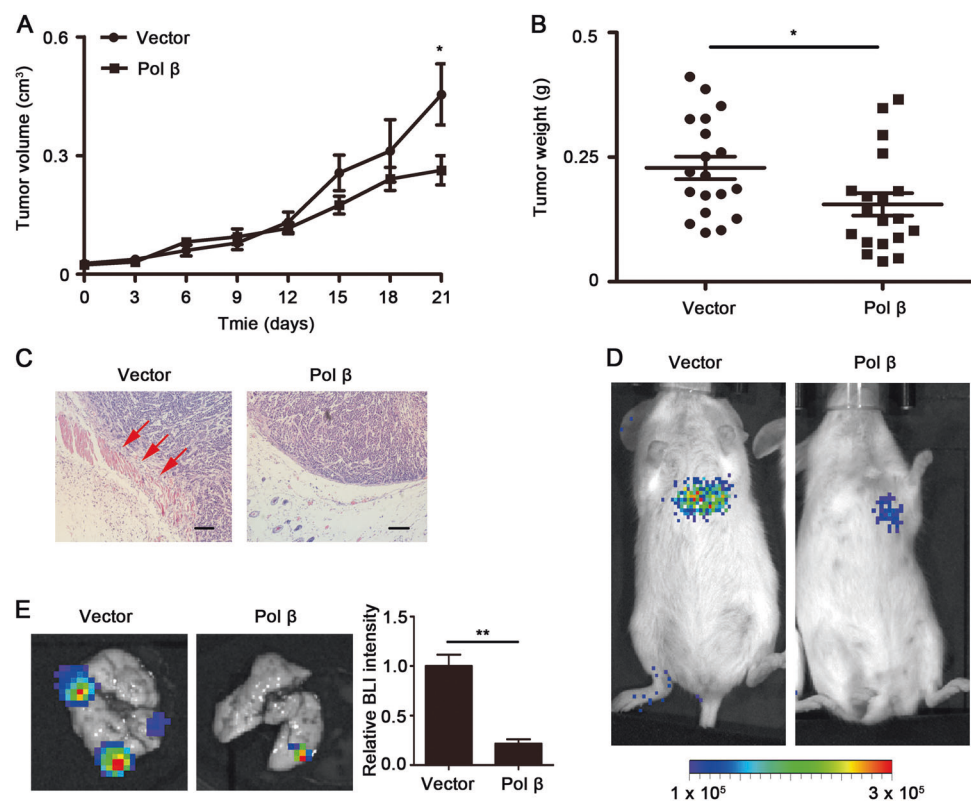
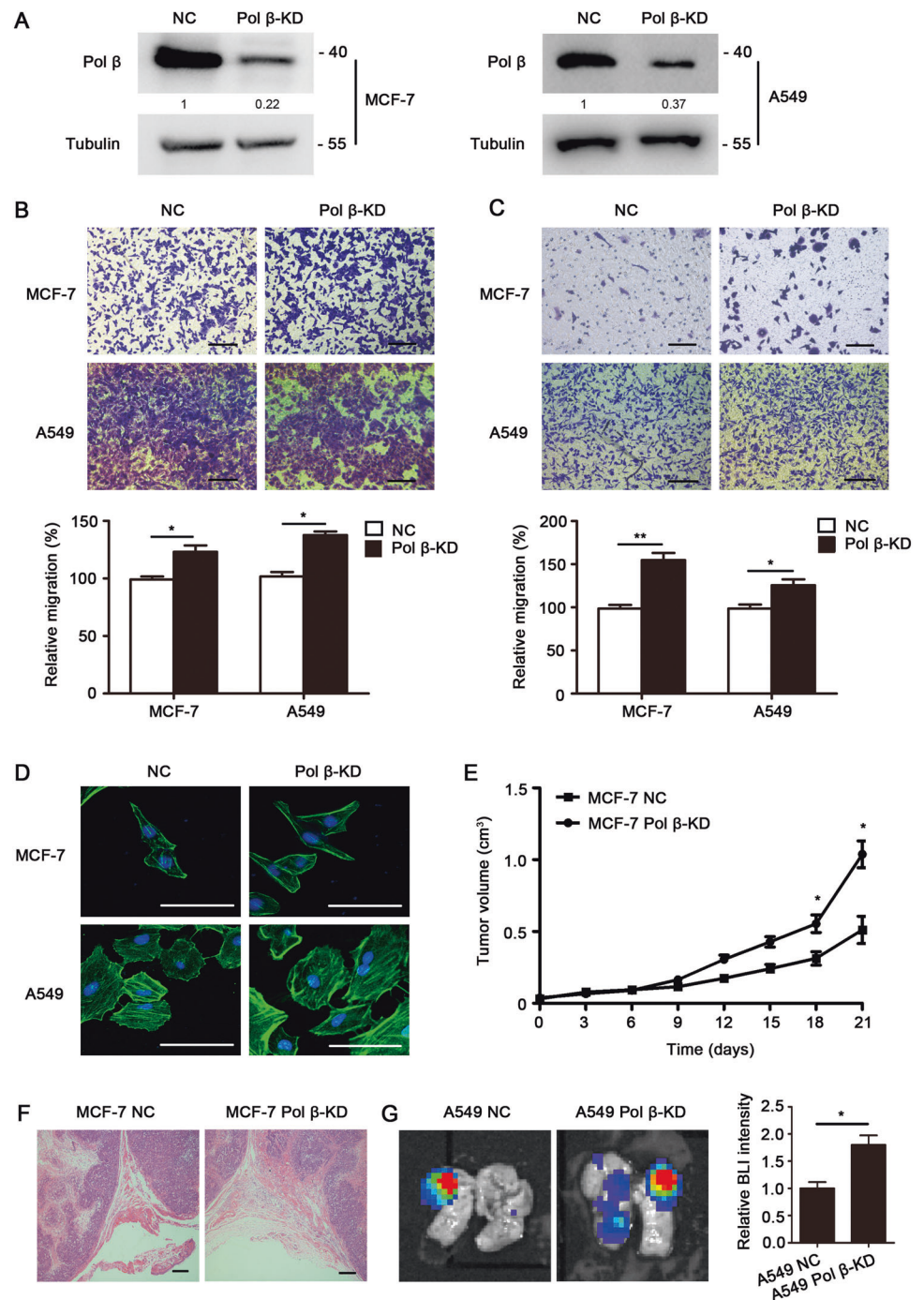


**Fig. 3 Deficiency of Pol  $\beta$  enhances tumor metastasis.** **a** Pol  $\beta$  was knocked down in MCF-7 and A549 cells. Western blot analysis of protein levels of Pol  $\beta$ . Representative images of transwell assay for cell migration (**b**) and invasion (**c**) in MCF-7 and A549 cells. The bottom part shows the relative percentage compared with negative control (\*\* $P < 0.01$ , by Student's  $t$  test). **d** Actin stained with phalloidin (green) showed cell spreading in MCF-7 and A549 cells. **e** MCF-7 cells containing vector or Pol  $\beta$  shRNA were injected subcutaneously. Tumor growth were measured every 3 days ( $n = 10$ ) (\* $P < 0.05$ , by Student's  $t$  test). **f** Tumors were collected and stained with H&E to test tumor invasion. **g** Representative bioluminescent (BLI) images of SCID mice after intravenous injection with A549-vector and A549 knockdown Pol  $\beta$  cells ( $n = 5$ ). The quantification of bioluminescence imaging signals was showed in right. (\* $P < 0.05$ , by Student's  $t$  test).



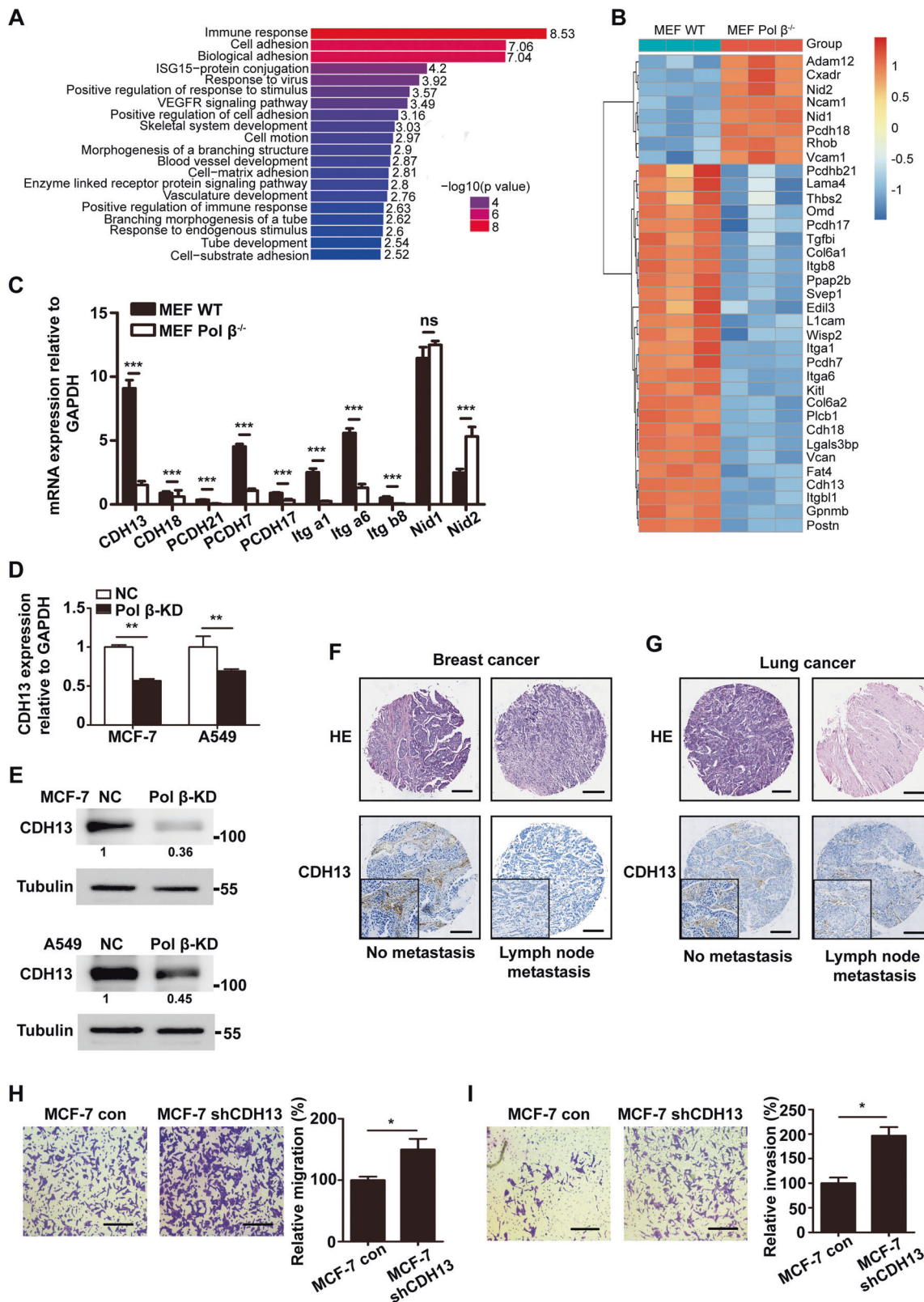
### Pol $\beta$ suppresses cancer migration and invasion by regulating gene expression of CDH13

As mentioned above, Pol  $\beta$  is relevant to cancer invasion and metastasis. These results promote us to investigate the genes involved in the Pol  $\beta$ -dependent cancer metastasis. Using microarray, gene expression profiles were analyzed with wild-type (WT) MEF and Pol  $\beta^{-/-}$  MEF cells that were well characterized as a Pol  $\beta$  deficient cell line. Total

522 genes showed significant changes more than twofolds ( $P < 0.05$ ) in Pol  $\beta^{-/-}$  MEF cells. Among these, 386 genes were downregulated and 136 genes were upregulated in Pol  $\beta$  knockout MEF cells versus WT MEF cells;  $P < 0.05$  (Supplementary Table 2). To characterize the enriched biological processes in our microarray, the 522 genes were subjected to gene ontology (GO) enrichment analysis. The genes involved in immune response and cell adhesion were amply presented (Fig. 4a). Among the genes involved in

cell adhesion, 27 genes were downregulated and 5 genes were upregulated in Pol  $\beta^{-/-}$  MEF cells compared those in WT MEF cells (Fig. 4b). Real-time PCR (qRT-PCR)

confirmed the downregulation of CDH13, CDH18, PCDH7, PCDH17, PCDH21, Itg  $\alpha 1$ , Itg  $\alpha 6$ , and Itg  $\beta 8$ , and upregulation of Nid1 and Nid2 in Pol  $\beta^{-/-}$  MEF cells (Fig. 4c).





◀ **Fig. 4 Pol  $\beta$  suppresses cancer cell migration by regulating gene expression of CDH13.** **a** GO analysis in Pol  $\beta$  null MEF cells compared with WT MEF cells. **b** The heat map represents the expression level of gene significantly changed in Pol  $\beta$  null MEF cells. **c** qRT-PCR analysis of mRNA level of several cadherins family members in MEF cells (\*\* $P < 0.01$ , by Student's  $t$  test). **d** qRT-PCR analysis of mRNA level of CDH13 in Pol  $\beta$  knock down MCF-7 and A549 cells (\*\* $P < 0.01$ , by Student's  $t$  test). **e** Western blot analysis of protein level of CDH13 in MCF-7 cells and A549 cells. Representative images of HE staining and (IHC) staining of CDH13 in tumor tissues of breast tumor (**f**) and lung tumor (**g**). Transwell assay for cell migration (**h**) and invasion (**i**) in MCF-7 cells. Representative images are shown in the left panel and relative percentage compared with control is shown in the right panel (\*\* $P < 0.05$ , by Student's  $t$  test).

Our data showed that CDH13 was one of top-five genes regulated in Pol  $\beta^{-/-}$  MEF cells (Fig. 4b). Moreover, CDH13 was a predominant cell adhesion gene with high expression level in cells (Fig. 4c). We confirmed the effect of Pol  $\beta$  levels on modulation of the CDH13 expression. Overexpression of Pol  $\beta$  restored CDH13 expression in Pol  $\beta^{-/-}$  MEF cells (Fig. S5a). Downregulation of *CDH13* mRNA levels was also detected in Pol  $\beta$  deficient MCF-7 and A549 cells (Fig. 4d), as well as CDH13 protein levels (Fig. 4e). Moreover, overexpression of Pol  $\beta$  promoted expression of CDH13 in both MCF-7 and A549 cells (Fig. S5b, c).

Literature review and analysis indicated that CDH13 profoundly affected cancer metastasis, tumor progression, and tumor angiogenesis [31]. To evaluate the regulatory effect of CDH13 on cancer cell migratory and invasive capabilities, the protein expression level of CDH13 was assessed in both breast and lung cancer tissue samples using tissue array analysis. The data showed that lower expression of CDH13 was associated with higher lymph node metastases in both breast cancer and lung cancer (Fig. 4f, g). Furthermore, transwell assay demonstrated that knockdown of CDH13 promoted MCF-7 cell migration and invasion (Fig. 4h, i and Fig. S6a). Collectively, these data confirmed that CDH13 was a negative regulator in cancer metastasis.

### Suppression of tumor cell motility in Pol $\beta$ deficient cells depends on CDH13

To further investigate the possible involvement of CDH13 in Pol  $\beta$  regulated cancer cell migration and invasion, CDH13 was knockdown by shRNA lentiviruses in Pol  $\beta$ -overexpressing MCF-7 cells (Fig. S6b). Transwell assay showed that cell migratory and invasive capabilities were significantly increased after knockdown of CDH13 in Pol  $\beta$ -overexpressing MCF-7 cells (Fig. 5a, b). Xenograft tumors derived from Pol  $\beta$ -overexpressing MCF-7 cells with CDH13 shRNA showed a higher growth rate compared with those derived from control Pol  $\beta$ -overexpressing MCF-7 cells (Fig. 5c). Consistently, knockdown of CDH13 restored

the final tumor weight in Pol  $\beta$ -overexpressing tumor (Fig. 5d). In addition, IHC analysis showed that Knockdown of CDH13 promoted tumor local invasion as well (Fig. 5e).

### Deletion of CDH13 restores the repressed angiogenesis by Pol $\beta$

Angiogenesis is one of the hallmarks in cancer, which is required for invasive tumor growth and metastasis by providing oxygen and nutrients for tumor cells [32]. The previous research reported that CDH13 downregulation in cancerous cells may promote neovascularization [33]. We elucidated the effect of Pol  $\beta$  and CDH13 on tumor angiogenesis. Tumors derived from Pol  $\beta$ -overexpressing MCF-7 cells showed the smaller size and less blood capillary compared with tumors derived from WT MCF-7 cells, whereas knockdown of CDH13 restored the angiogenesis and hemoglobin content in Pol  $\beta$ -overexpressing tumors (Fig. 6a, b). CD31 staining also revealed a decrease in tumor microvessel density in Pol  $\beta$ -overexpressing tumors, which was rescued by knockdown of CDH13 (Fig. 6c). In addition, the expression of genes including VEGFA, VEGFR2, and FGF $\beta$ , which were associated with angiogenesis, was detected repressed. Our data showed that overexpression of Pol  $\beta$  repressed these genes expression, and knockdown of CDH13 in Pol  $\beta$ -overexpressing tumors rescued the expression levels of these genes (Fig. 6d). These results further demonstrated that deficiency of Pol  $\beta$  had an effect on many genes that are hallmarks of cancer.

### Pol $\beta$ promotes CDH13 expression through promoting DNA demethylation of CDH13 promoter

We next sought to identify the mechanism of regulation of CDH13 gene expression by Pol  $\beta$ . Functional downregulation of DNA repair genes may impair repair of endogenous DNA damage and further aggravation of the load of DNA damage, leading to genomic instability and abnormal gene expression [34, 35]. To investigate whether the role of Pol  $\beta$  in regulation of CDH13 expression is due to the accumulated DNA damage in Pol  $\beta$  knocking-down (KD) cells, we detected  $\gamma$ H2AX levels in Pol  $\beta$  KD MCF-7 cell and found that the  $\gamma$ H2AX levels showed no differences between WT and Pol  $\beta$  KD cells (Fig. S7a). Our results were supported by a functional deficiency of Pol  $\beta$  mutant P242R, which showed no effect on DNA damage accumulation in cells without MMS treatment [36]. Moreover, the comet assay showed that slightly increasing chromosome damage was detected in MCF-7 Pol  $\beta$  KD cells compared with WT MCF-7 cells without MMS treatment (Fig. S7b). However, MMS treatment augmented average comet tail length in Pol  $\beta$  KD MCF-7 cells compared with that in WT MCF-7 cells, indicating that the knockdown of

**Fig. 5 Pol  $\beta$  suppression of tumor cell motility depends on CDH13.** Transwell assay for cell migration (a) and invasion (b) in MCF-7 con, MCF-7 overexpression Pol  $\beta$  and knockdown CDH13 in Pol  $\beta$  overexpressed MCF-7 cells. Representative images are shown in the left panel and relative percentage compared with control is shown in the right panel (\*\* $P < 0.01$ , by Student's  $t$  test). Tumor growth (c) and weight (d) were measured after subcutaneous injection ( $n = 6$ ) ( $*P < 0.05$ , by two Student's  $t$  test). e Representative images of HE assay indicated tumor local invasion.

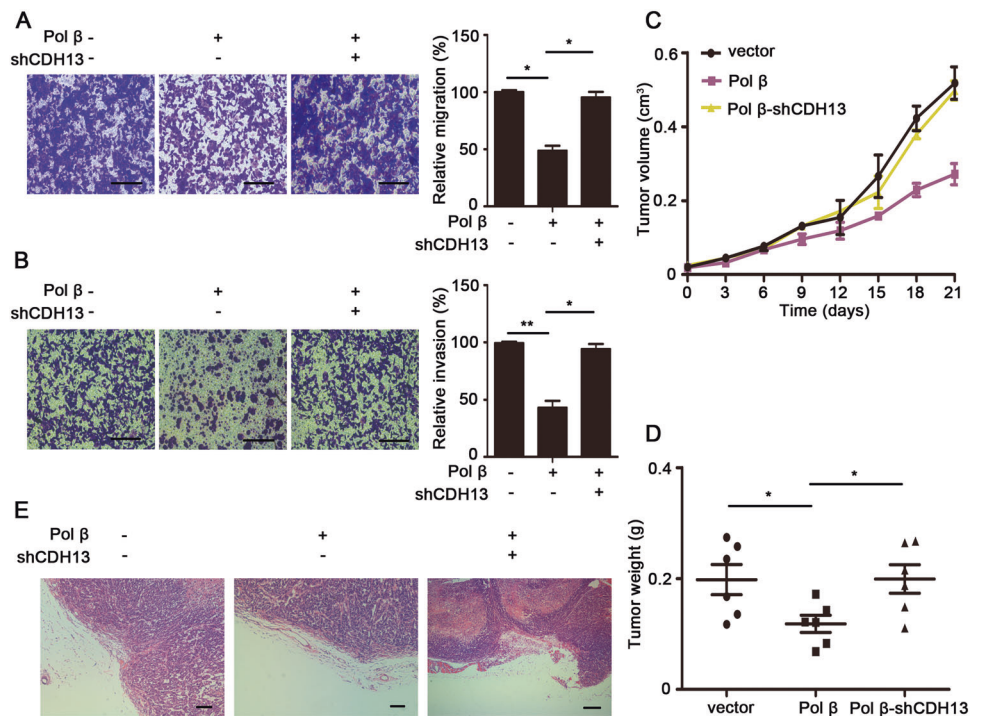
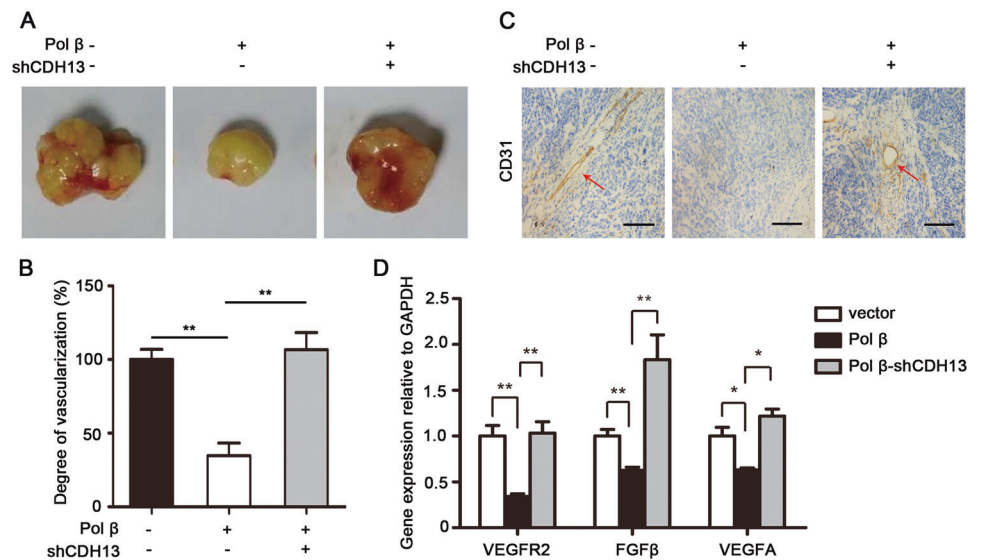


**Fig. 6 Deletion of CDH13 restores the repressed angiogenesis by Pol  $\beta$ .** a Typical tumors from nude mice after subcutaneous injection. b Neovascularization of tumor measured by the Drabkin's reagent kit. (\*\* $P < 0.01$ , by Student's  $t$  test). c Representative micrographs of CD31 IHC staining of assay of tumor samples. d qRT-PCR analysis gene expression involved in angiogenesis ( $*P < 0.05$ , \*\* $P < 0.01$ , by Student's  $t$  test).



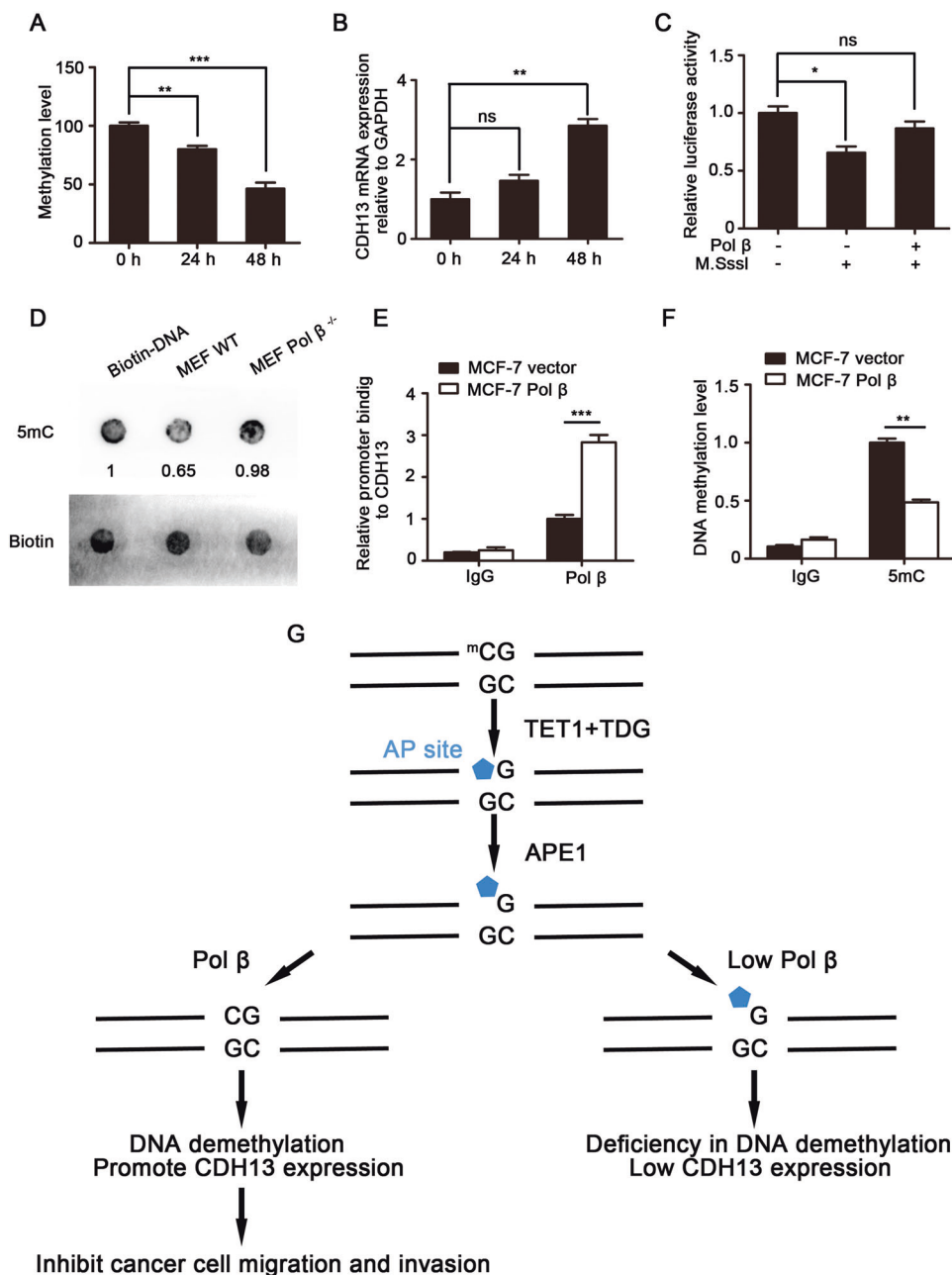
Pol  $\beta$  reduced the BER activity in cells (Fig. S7b). Furthermore, we detected the regulation of CDH13 expression under DNA damage stress. Both WT and Pol  $\beta$  KD MCF-7 cells were treated with 2  $\mu$ M MMS for 1 h followed by recover periods for 0, 1, 3, or 6 h. Expectedly, there was an increase of the  $\gamma$ H2AX levels until 3-h recovery in both cell lines following MMS treatment, and knockout of Pol  $\beta$  enhanced the increasing  $\gamma$ H2AX levels. The protein levels of Pol  $\beta$  and CDH13 were also increased in WT MCF-7 cells with MMS treatment followed by a recovery 1 or 3 h; however, the CDH13 protein levels showed no changes in

Pol  $\beta$  KD MCF-7 cells after MMS treatment (Fig. S7c). The similar results were also obtained with continuous treatments by MMS from 0.5 to 6 h (Fig. S7d). Furthermore, to detect if the endogenous damage caused by DNA repair deficiency could regulate CDH13 expression, we knocked down another key DNA repair factor XRCC1 (Fig. S8a), whose absence contributes to the spontaneously persistence of DNA strand breaks [37]. Our data showed that knockdown of XRCC1 have no effect on CDH13 expression, while the DNA damage marker  $\gamma$ H2AX was significantly upregulated by knockdown of XRCC1 (Fig. S8b).



**Fig. 7 Pol  $\beta$  impedes DNA methylation of CDH13 promoter leading to promote CDH13 expression. a**

**MethylLight analysis of the CDH13 promoter in cells after treated with 5  $\mu$ M decitabine (\*\* $P$  < 0.01, \*\*\* $P$  < 0.001, by Student's  $t$  test). **b** Quantitative real-time PCR analysis of CDH13 expression after decitabine treatment (\*\* $P$  < 0.01, by Student's  $t$  test). **c** luciferase assay using pGL3 reporter system with the CDH13 promoter. The firefly luciferase activity of each sample normalized to the *Renilla* luciferase (internal control) (\* $P$  < 0.05, by Student's  $t$  test). **d** Biotin-labeled DNA was incubated with whole cell extract and tested by dot blot. **e** ChIP assay for the enrichment of CDH13 promoter in MCF-7 expressed vector and Pol  $\beta$  cells. IgG used as a negative control. **f** Methylation ChIP assay for the enrichment of CG region in cells as in **e** (\*\* $P$  < 0.01, \*\*\* $P$  < 0.001, by Student's  $t$  test). **g** Schematic of the role of Pol  $\beta$  in DNA demethylation of CDH13 promoter and cancer metastasis.**



Several studies showed that CDH13 promoter DNA methylation regulates its expression and that is correlated with cancer prognosis and diagnosis [18]. In agreement with these data, using decitabine to inhibit DNA methylation, we demonstrated that DNA methylation levels of CDH13 promoter regulate CDH13 expression (Fig. 7a, b). BER has been previously implicated in active demethylation, in which Pol  $\beta$  plays a key role [38–40]. Thus, we hypothesized that downregulation of Pol  $\beta$  affects CDH13 expression through modulating its promoter DNA methylation. Indeed, luciferase assay using pGL3 system with CDH13 promoter showed that activity of CDH13 promoter was repressed when it was methylated by CpG methylase M. SssI, and could be

restored by overexpression of Pol  $\beta$  (Fig. 7c). Furthermore, in vitro demethylation assay using whole cell extract with/without Pol  $\beta$  showed that knockout of Pol  $\beta$  remarkably impaired the DNA demethylation activity of whole cell extract (Fig. 7d). Furthermore, quantitative chromatin immunoprecipitation (ChIP) assays showed that Pol  $\beta$  bound directly to the promoter region of CDH13 (Fig. 7e). We assessed DNA methylation levels of CDH13 promoter by MeDIP-qPCR assay, and found that higher methylation level of CDH13 promoter in WT MCF-7 cell compared with Pol  $\beta$ -overexpressing MCF-7 cell (Fig. 7f). Our results suggested that Pol  $\beta$  regulated CDH13 gene expression through regulating its promoter DNA demethylation level.

## Discussion

In this study, we report a role of Pol  $\beta$  in repressing cancer cell metastasis and invasion during cancer progression. Our data show that the expression levels of Pol  $\beta$  are associated with the lymph node metastases status in both breast cancer and lung cancer. Overexpression of Pol  $\beta$  remarkably impeded cancer cell migratory and invasive capabilities, whereas deficiency of Pol  $\beta$  promotes these capabilities. Moreover, our data suggest that the function of Pol  $\beta$  on repressing tumor migration and invasion is dependent on upregulation of CDH13 expression by promoting DNA demethylation of CDH13 promoter.

Pol  $\beta$ , a key enzyme involved in BER, plays multiple biological roles in tumor growth, cell transformation and tumorigenesis [36, 41]. Pol  $\beta$  has been implicated in clinical outcomes and survival of tumor patients [24, 25]. Consistently, we found that the higher expression of Pol  $\beta$  was associated with less lymphatic metastasis and better patient survival. Accordingly, overexpression of Pol  $\beta$  inhibits cancer cell migration and invasion both in vitro and in vivo. Our results implicate Pol  $\beta$  in the regulation of cancer cell migratory and invasive capabilities during cancer progression.

Cellular invasion and migration are governed by extracellular and intracellular signals, and depend on the interaction of the surrounding cells and ECM [10]. To characterize the molecular mechanism of Pol  $\beta$ -regulating cancer metastasis, we determine the change of gene expression profile in Pol  $\beta$ -deleted cell context. The genes involved in cell adhesion including cadherin superfamily were significantly modified after knockout of Pol  $\beta$ . CDH13 is an atypical cadherin, which shows function on inhibiting cancer cell proliferation and invasiveness, and increasing susceptibility to cell apoptosis, resulting in reduction of tumor growth [15, 16]. Real-time qPCR and western blot analysis demonstrate the regulation of CDH13 expression by Pol  $\beta$ . Furthermore, knockdown of CDH13 reverses the effect of Pol  $\beta$  on tumor metastasis repression.

It has been reported that tumor growth and progression is limited until the vascularization of the neoplastic mass [42]. Vascularization is achieved via neoangiogenesis and co-option of existing blood vessels or a combination of these processes. Metastasis then occurs when invading tumor cells engage with blood and lymph vessels, penetrates basement membranes and endothelial walls, and disseminates to colonize distant organs [43]. In agreement with preceding observations, we found that overexpression of Pol  $\beta$  could depress angiogenesis in tumor progression, whereas down-regulation of CDH13 could restore this process. These results indicated that the effects of Pol  $\beta$  on cancer cell invasion and migration are also through repressing angiogenesis. These data indicate that Pol  $\beta$  impedes tumor metastasis at least partially via promoting CDH13 expression.

Pol  $\beta$  plays a critical role in BER and the reduced activity of Pol  $\beta$  impairs efficiency of BER [2, 22]. The comet assay indicated that Pol  $\beta$  KD MCF-7 cell has lower activity of DNA repair after MMS treatment. However, knockdown of Pol  $\beta$  has no effect on the accumulation of the endogenous DNA damage levels in cells without exogenous DNA damage reagent treatment. Furthermore, the expression of CDH13 showed no significant change in Pol  $\beta$  KD MCF-7 cells with MMS treatment. Numerous evidences suggest that the expression of CDH13 is regulated by DNA methylation of its promoter [17]. A current model indicates that BER is involved in TET1–TDG–BER-mediated DNA demethylation [39]. In this model, 5mC can be oxidated to 5fC and 5caC by TET1. The interaction between TET1 and TDG implicates a link between 5mC oxidation and base excision. The BER pathway is required for AP-site repair generated by TDG. Moreover, the activity of BER was linked to active global DNA demethylation, and BER proteins were reported to be involved in DNA demethylation pathway [44–46]. Our in vitro methylation assay provided evidence that the expression of CDH13 is regulated by the DNA methylation levels of its promoter. In addition, we observed that the DNA methylation levels of CDH13 promoter is lower in Pol  $\beta$ -overexpressing cells compared with those in WT cells, indicating that Pol  $\beta$  is involved in regulation of methylation levels of CDH13 promoter. Our ChIP assay indicated the directly binding of Pol  $\beta$  to CDH13 promoter. Collectively, Pol  $\beta$  could affect the DNA demethylation of CDH13 promoter in TET1-BER pathway (Fig. 7g).

In conclusion, we uncovered a novel role of Pol  $\beta$  in cancer progression that Pol  $\beta$  repress tumor metastasis by promoting CDH13 expression. Our results rise the possibility that cancer patients with metastasis might benefit from stimulation but not inhibition of Pol  $\beta$  as its function on repression of tumor metastasis.

## Materials and methods

### Cell culture and stable cell lines

MCF-7 cells, A549 cells, and H293 cells were obtained from the Institute of Cell Biology (Chinese Academy of Science, Shanghai, China) and cultured in DMEM medium supplemented with 10% fetal bovine serum (FBS) and 1% penicillin/streptomycin. For Pol  $\beta$ -overexpressing MCF-7 and A549 stable cells, cells were infected by purified lentivirus for 48 h and then selected by puromycin for 7 days.

For knockdown Pol  $\beta$  and CDH13, we used lentivirus vector pGLV3 containing a shRNA sequence. The follow oligonucleotides were used: human Pol  $\beta$  shRNA: 5'-GAGCTGAAGCTAAGAAATTG-3'; human CDH13 shRNA: 5'-AGAAAGTGTTCATATCAACTC-3'. MEF

Pol  $\beta$  knockout cell and corresponding littermate WT control cell were a kindly provided by Dr. Binghui Shen (Beckman Research Institute, City of Hope, Duarte, CA, USA). All cell lines were found to be negative for mycoplasma contamination.

### Quantitative real-time PCR

Total RNA from cells and tissues were isolated by TRIzol reagent (Invitrogen) and reverse transcribed into cDNA. Quantitative real-time PCR was performed using SYBR Green (Vazyme Biotech, China, Q341-02) and operated on ABI StepOne. Each reaction was repeated three times. Gene relative expression was determined relative to GAPDH in each reaction. The relative amounts of mRNA were calculated using the comparative cycle threshold method ( $2^{-\Delta\Delta Ct}$ ) [1]. The primers for RT-PCR are listed in Supplementary Table 1.

### Western blot analysis and antibodies

Total cellular protein was extracted by RIPA buffer and subjected to SDS-PAGE gel. Protein then was transferred to polyvinylidene difluoride membranes. After blocking, the membranes were incubated overnight at 4 °C with primary antibody. The membranes were incubated with secondary antibody following extensive washing. Blot was filmed by enhanced chemiluminescence and developed via Tanon-4500 luminescent imaging workstation (Tanon Science & Technology, Shanghai, China). The following antibodies were used for western blotting: Pol  $\beta$  (ab175197, Abcam) and CDH13 (ab167407, Abcam)

### Immunofluorescence assays

For immunofluorescence assays, cells were washed with PBS for three times then fixed with 4% formaldehyde for 10 min at room temperature. After permeabilization with 0.1% Triton X-100 for 10 min, cells were blocked with 3% BSA for 1 h. Then, cells were incubated with indicated primary antibodies overnight at 4 °C. Following washed with PBST for three times, cells were incubated with fluorescent secondary antibodies for 2 h at room temperature. Subsequently, cells were stained with DAPI and visualized under a fluorescence microscope (Nikon 80I 10-1500 $\times$ ).

### IHC assays

Immunohistochemical staining was performed as previously described [3]. Briefly, tissues were fixed in 10% formalin. Paraffin-embedded sections from tissue specimens were deparaffinized and heated at 97 °C in 10 mM citrate buffer

(pH 6.0) for 20 min for antigen retrieval. Slides were incubated with primary antibody at 4 °C overnight, followed by incubation with secondary antibody at room temperature and visualized using a DAB Kit (Invitrogen). The expression levels of target proteins in tissue were examined according to the semiquantitative immunoreactivity score (IRS) [27]. Accordingly, category A documented the intensity of immunostaining as 0–3 (0, negative; 1, weak; 2, moderate; 3, strong). Category B documented the percentage of immunoreactive cells as 1 (0–25%), 2 (26–50%), 3 (51–75%), and 4 (76–100%). Multiplication of category A and B resulted in an IRS ranging from 0 to 12 for each no lymph node status metastasis tumor or lymph node status metastasis tumor. Expression of protein levels in tissue with  $IRS \leq 6$  were classified as low expression and which in samples with  $IRS > 6$  were classified as high expression.

### 3D matrigel assay

Firstly, matrigel was spread on a 12-well plate. Cells were trypsinized into single cells and plated into the well with matrigel. After incubation at 37 °C for about 20 min, top medium was replaced with growth medium containing 5% matrigel. Fresh medium with 5% matrigel was changed every 2 days. Cells were cultured for 6–8 days before analysis.

### Cell migration and invasion assays

Cell migration and invasion assays were analyzed by using wound healing and transwell assays. For the wound healing assay, cells plated on a six-well plate were scratched by a pipette tip. Cells were washed with PBS and cultured in serum-free medium. Photos were taken at indicated times.

For transwell assays, cells were trypsinized into single cells and seeded into the upper chamber of the transwell apparatus (Corning Costar) in serum-free medium. Medium with 20% FBS was added into the bottom chamber. After 12–16 h, cells passed through the polycarbonate filter were stained by 0.5% crystal violet for 10 min. For cell invasion assay, matrigel was used to precoat the upper chamber firstly, and then cells were seeded into the upper chamber of the transwell apparatus.

### DNA methylation analysis

MCF-7 cells were treated with decitabine (MCE). Genomic DNA was isolated by QIAamp DNA Mini Kit (51304). Sodium bisulfite conversion of genomic DNA was performed using the EZ DNA Methylation Kit (Zymo Research; D5002). After sodium bisulfite conversion, the genomic DNA was amplified by qPCR. The primers used are listed in Supplementary Table 1.



## CDH13 promoter reporter analysis

Luciferase activity was assessed according to previous report [1]. CDH13 promoter was cloned into pGL3-basic reporter vector and methylated by incubation with CpG methylase M. SssI (Zymo Research). H293 cells were cotransfected with plasmids on a 24-well plate. Thirty-six hours after transfection, cells were harvested for firefly and *Renilla* luciferase activity assays. The *Renilla* luciferase activities were used to normalize the transfection efficiency.

## ChIP assay

ChIP assays were performed following the protocol of ChIP kit (Cell Signaling Technology, 9002s). ChIP samples were analyzed by quantitative real-time PCR. DNA copies in immunoprecipitation samples were normalized to input DNA control samples. For DNA methylation ChIP assay, purified DNA in IP buffer was sonicated to make fragment DNA size between 300 and 800 bp. Two micrograms of 5 mC antibody (Abcam, ab10805) was added into a final volume of 500  $\mu$ l IP buffer with fragment DNA, followed by rotating incubation at 4 °C overnight. Fragment DNA with 5 mC antibody was pulled down by protein A/G agarose for 2 h and purified by DNA purification kit. The primer sequences for ChIP-qPCR assay are listed in Supplementary Table 1.

## In vivo tumor analysis

All animal experiments were performed according to the procedures approved by the Laboratory Animal Care Committee at Nanjing Normal University and followed National Institutes of Health guide for the care and use of Laboratory animals. Mice were purchased from the Model Animal Research Center of Nanjing University (Nanjing, China), and were maintained under specific pathogen-free conditions. Six-to-seven weeks old female nude mice were used for subcutaneous inoculation. Cells were trypsinized and resuspended in DMEM with 50% matrigel at a consistence of  $1 \times 10^7$  cells/ml. A total of  $1 \times 10^6$  cells were injected into flank of mice. Tumor volume was measured twice a week until fifth week. For lung cancer metastasis assay, female SCID mice were used for lateral tail vein injection with  $1 \times 10^6$  A549 cells (luciferase labeled) per mice. Four weeks after injection, lung nodules and progression were monitored and quantified using the bioluminescence system (Caliper IVIS Lumina XR).

## Statistical analysis

Statistical analysis was performed with GraphPad Prism 6.0. Statistical significance was determined using two-tailed

Student's *t* test or analysis of variance in the case of comparisons among more than two groups. *P* values less than 0.05 were considered as significant.

**Acknowledgements** The authors would like to thank Dr. Binghui Shen (Beckman Research Institute, City of Hope, Duarte, CA, USA) for the MEF cell lines. This work was supported by the National Natural Science Foundation of China (81872284), the Natural Science Foundation of Colleges and Universities in Jiangsu Province (19KJA180010), and the Priority Academic Program Development of Jiangsu Higher Education Institutions.

## Compliance with ethical standards

**Conflict of interest** The authors declare that they have no conflict of interest.

**Publisher's note** Springer Nature remains neutral with regard to jurisdictional claims in published maps and institutional affiliations.

## References

- Lu X, Liu R, Wang M, Kumar AK, Pan F, He L, et al. MicroRNA-140 impedes DNA repair by targeting FEN1 and enhances chemotherapeutic response in breast cancer. *Oncogene*. 2020;39:234–47.
- Zhou T, Pan FY, Cao Y, Han Y, Zhao J, Sun HF, et al. R152C DNA Pol beta mutation impairs base excision repair and induces cellular transformation. *Oncotarget*. 2016;7:6902–15.
- Wang M, Li E, Lin L, Kumar AK, Pan F, He L, et al. Enhanced activity of variant DNA polymerase beta (D160G) contributes to cisplatin therapy by impeding the efficiency of NER. *Mol Cancer Res*. 2019;17:2077–88.
- Broustas CG, Lieberman HB. DNA damage response genes and the development of cancer metastasis. *Radiat Res*. 2014;181:111–30.
- Rytelewski M, Tong JG, Buensuceso A, Leong HS, Maleki Vareki S, Figueredo R, et al. BRCA2 inhibition enhances cisplatin-mediated alterations in tumor cell proliferation, metabolism, and metastasis. *Mol Oncol*. 2014;8:1429–40.
- Wiegman AP, Al-Ejeh F, Chee N, Yap PY, Gorski JJ, Da Silva L, et al. Rad51 supports triple negative breast cancer metastasis. *Oncotarget*. 2014;5:3261–72.
- Choi EB, Yang AY, Kim SC, Lee J, Choi JK, Choi C, et al. PARP1 enhances lung adenocarcinoma metastasis by novel mechanisms independent of DNA repair. *Oncogene*. 2016;35:4569–79.
- Eccles SA, Welch DR. Metastasis: recent discoveries and novel treatment strategies. *Lancet*. 2007;369:1742–57.
- Valastyan S, Weinberg RA. Tumor metastasis: molecular insights and evolving paradigms. *Cell*. 2011;147:275–92.
- Lu P, Weaver VM, Werb Z. The extracellular matrix: a dynamic niche in cancer progression. *J Cell Biol*. 2012;196:395–406.
- Pignatelli M, Vessey CJ. Adhesion molecules: novel molecular tools in tumor pathology. *Hum Pathol*. 1994;25:849–56.
- Makrilia N, Kollias A, Manolopoulos L, Syrigos K. Cell adhesion molecules: role and clinical significance in cancer. *Cancer Investig*. 2009;27:1023–37.
- Nollet F, Kools P, van Roy F. Phylogenetic analysis of the cadherin superfamily allows identification of six major subfamilies besides several solitary members. *J Mol Biol*. 2000;299:551–72.
- Gugnoni M, Sancisi V, Gandolfi G, Manzotti G, Ragazzi M, Giordano D, et al. Cadherin-6 promotes EMT and cancer metastasis by restraining autophagy. *Oncogene*. 2017;36:667–77.

15. Chan DW, Lee JM, Chan PC, Ng IO. Genetic and epigenetic inactivation of T-cadherin in human hepatocellular carcinoma cells. *Int J Cancer*. 2008;123:1043–52.
16. Kuphal S, Martyn AC, Pedley J, Crowther LM, Bonazzi VF, Parsons PG, et al. H-cadherin expression reduces invasion of malignant melanoma. *Pigment Cell Melanoma Res*. 2009;22:296–306.
17. Ye M, Huang T, Li J, Zhou C, Yang P, Ni C, et al. Role of CDH13 promoter methylation in the carcinogenesis, progression, and prognosis of colorectal cancer: A systematic meta-analysis under PRISMA guidelines. *Medicine*. 2017;96:e5956.
18. Chen F, Huang T, Ren Y, Wei J, Lou Z, Wang X, et al. Clinical significance of CDH13 promoter methylation as a biomarker for bladder cancer: a meta-analysis. *BMC Urol*. 2016;16:52.
19. Nicolay NH, Helleday T, Sharma RA. Biological relevance of DNA polymerase beta and translesion synthesis polymerases to cancer and its treatment. *Curr Mol Pharmacol*. 2012;5:54–67.
20. Yamtich J, Sweasy JB. DNA polymerase family X: function, structure, and cellular roles. *Biochim et Biophys Acta*. 2010;1804:1136–50.
21. Li J, Luthra S, Wang XH, Chandran UR, Sobol RW. Transcriptional profiling reveals elevated Sox2 in DNA polymerase ss null mouse embryonic fibroblasts. *Am J Cancer Res*. 2012;2:699–713.
22. Guo Z, Zheng L, Dai H, Zhou M, Xu H, Shen B. Human DNA polymerase beta polymorphism, Arg137Gln, impairs its polymerase activity and interaction with PCNA and the cellular base excision repair capacity. *Nucleic Acids Res*. 2009;37:3431–41.
23. Bergoglio V, Pillaire MJ, Lacroix-Triki M, Raynaud-Messina B, Canitrot Y, Bieth A, et al. Deregulated DNA polymerase beta induces chromosome instability and tumorigenesis. *Cancer Res*. 2002;62:3511–4.
24. Abdel-Fatah TM, Russell R, Agarwal D, Moseley P, Abayomi MA, Perry C, et al. DNA polymerase beta deficiency is linked to aggressive breast cancer: a comprehensive analysis of gene copy number, mRNA and protein expression in multiple cohorts. *Mol Oncol*. 2014;8:520–32.
25. Matakidou A, el Galta R, Webb EL, Rudd MF, Bridle H, Eisen T, et al. Genetic variation in the DNA repair genes is predictive of outcome in lung cancer. *Hum Mol Genet*. 2007;16:2333–40.
26. Tan X, Wu X, Ren S, Wang H, Li Z, Alshenawy W, et al. A point mutation in DNA polymerase beta (POLB) gene is associated with increased progesterone receptor (PR) expression and intraperitoneal metastasis in gastric cancer. *J Cancer*. 2016;7:1472–80.
27. Ju J, Chen A, Deng Y, Liu M, Wang Y, Wang Y, et al. NatD promotes lung cancer progression by preventing histone H4 serine phosphorylation to activate Slug expression. *Nat Commun*. 2017;8:928.
28. Zheng W, Li J, Wang X, Yuan Y, Zhang J, Xiu Z. Effects of Antarctic krill docosahexaenoic acid on MCF-7 cell migration and invasion induced by the interaction of CD95 with caveolin-1. *Life Sci*. 2018;192:270–7.
29. Vens C, Dahmen-Mooren E, Verwijs-Janssen M, Blyweert W, Graversen L, Bartelink H, et al. The role of DNA polymerase beta in determining sensitivity to ionizing radiation in human tumor cells. *Nucleic Acids Res*. 2002;30:2995–3004.
30. Weed SA, Parsons JT. Cortactin: coupling membrane dynamics to cortical actin assembly. *Oncogene*. 2001;20:6418–34.
31. Andreeva AV, Kutuzov MA. Cadherin 13 in cancer. *Genes Chromoso Cancer*. 2010;49:775–90.
32. Weis SM, Cheresh DA. Tumor angiogenesis: molecular pathways and therapeutic targets. *Nat Med*. 2011;17:1359–70.
33. Rubina K, Kalinina N, Potekhina A, Efimenko A, Semina E, Poliakov A, et al. T-cadherin suppresses angiogenesis in vivo by inhibiting migration of endothelial cells. *Angiogenesis*. 2007;10:183–95.
34. Fletcher SC, Grou CP, Legrand AJ, Chen X, Soderstrom K, Poletto M, et al. Sp1 phosphorylation by ATM downregulates BER and promotes cell elimination in response to persistent DNA damage. *Nucleic Acids Res*. 2018;46:1834–46.
35. Sun H, He L, Wu H, Pan F, Wu X, Zhao J, et al. The FEN1 L209P mutation interferes with long-patch base excision repair and induces cellular transformation. *Oncogene*. 2017;36:194–207.
36. Yamtich J, Nemecek AA, Keh A, Sweasy JB. A germline polymorphism of DNA polymerase beta induces genomic instability and cellular transformation. *PLoS Genet*. 2012;8:e1003052.
37. Levy N, Martz A, Bresson A, Spelnhauer C, de Murcia G, Menissier-de Murcia J. XRCC1 is phosphorylated by DNA-dependent protein kinase in response to DNA damage. *Nucleic Acids Res*. 2006;34:32–41.
38. He YF, Li BZ, Li Z, Liu P, Wang Y, Tang Q, et al. Tet-mediated formation of 5-carboxylcytosine and its excision by TDG in mammalian DNA. *Science*. 2011;333:1303–7.
39. Chen ZX, Riggs AD. DNA methylation and demethylation in mammals. *J Biol Chem*. 2011;286:18347–53.
40. Walsh CP, Xu GL. Cytosine methylation and DNA repair. *Curr Top Microbiol Immunol*. 2006;301:283–315.
41. Sobol RW. Genome instability caused by a germline mutation in the human DNA repair gene POLB. *PLoS Genet*. 2012;8:e1003086.
42. Bergers G, Benjamin LE. Tumorigenesis and the angiogenic switch. *Nat Rev Cancer*. 2003;3:401–10.
43. Fidler IJ. The pathogenesis of cancer metastasis: the 'seed and soil' hypothesis revisited. *Nat Rev Cancer*. 2003;3:453–8.
44. Weber AR, Krawczyk C, Robertson AB, Kusnierczyk A, Vagbo CB, Schuermann D, et al. Biochemical reconstitution of TET1-TDG-BER-dependent active DNA demethylation reveals a highly coordinated mechanism. *Nat Commun*. 2016;7:10806.
45. Hajkova P, Jeffries SJ, Lee C, Miller N, Jackson SP, Surani MA. Genome-wide reprogramming in the mouse germ line entails the base excision repair pathway. *Science*. 2010;329:78–82.
46. Schar P, Fritsch O. DNA repair and the control of DNA methylation. *Progress in drug research/Fortschritte der Arzneimittelforschung/Progres des recherches pharmaceutiques*. Beilin, Germany: Springer; 2011;67. p. 51–68.